

DESY 96-022

February 1996

SUSY-QCD Decays of Squarks and Gluinos

W. Beenakker^{1*}, R. Höpker², and P. M. Zerwas²

¹ Instituut-Lorentz, University of Leiden, The Netherlands

² Deutsches Elektronen-Synchrotron DESY, D-22603 Hamburg, Germany

ABSTRACT

The partial widths are determined for squark decays to gluinos and quarks, and gluino decays to squarks and quarks, respectively. The widths are calculated including one-loop SUSY-QCD corrections. The corrections amount to +30% to +50% for squark decays and -10% to +10% for gluino decays. We have derived the results in the \overline{DR} and \overline{MS} renormalization schemes, and we have demonstrated explicitly that the one-loop effective $q\bar{q}g$ and $q\tilde{q}\tilde{g}$ couplings are equal in the limit of exact supersymmetry.

*Research supported by a fellowship of the Royal Dutch Academy of Arts and Sciences

1 Introduction

The theoretical predictions for the decay properties of squarks and gluinos in supersymmetric theories are of interest for several reasons. The decay properties determine the experimental search techniques, and the measurement of decay branching ratios will allow us to study the couplings between the standard and the novel particles, interrelated by supersymmetry. A thorough analysis of the partial widths including higher-order corrections is required for this purpose at the theoretical level. SUSY-QCD corrections, which take into account the spectrum of the standard quarks/gluons and their supersymmetric partners squarks/gluinos, have so far been performed only for a few examples: The production of squark and gluino pairs at hadron colliders [1] and of squark pairs in e^+e^- annihilation [2], the decay of squarks to quarks and photinos [3], and the decay of charged Higgs bosons to stop/sbottom [4] and top/bottom particles [5]. In this note we present the theoretical predictions for the decay channels

$$\tilde{q} \rightarrow \tilde{g} + q \quad \text{for } m_{\tilde{q}} > m_{\tilde{g}} \quad (1)$$

$$\tilde{g} \rightarrow \tilde{q} + \bar{q} / \tilde{\bar{q}} + q \quad \text{for } m_{\tilde{g}} > m_{\tilde{q}} \quad (2)$$

including SUSY-QCD corrections. The analysis is performed for light quarks, excluding the case of top (s)quarks. This calculation is more demanding than the calculation for the decay processes discussed earlier in the literature due to the three colored particles involved in the initial and final states of (1) and (2). At the technical level, we will follow the path traced out for the production of squarks and gluinos in hadron collisions [1].

2 Theoretical Set-up

In analyzing the SUSY-QCD corrections, the supersymmetric squarks are assumed to be degenerate in mass. The formulae for squark decays apply to both chiral states, \tilde{q}_L and \tilde{q}_R . For gluino decays they include the sum over all flavor and chiral components and the two possible final states in Eq. (2) related by \mathcal{C} conjugation. The final states involving top quarks are not taken into account since we have treated the quarks in the final states as massless particles; the case of (s)top particles will be deferred to a subsequent analysis. In loops we have used a top-quark mass of $m_t = 180$ GeV and we have taken the top-squarks to be mass-degenerate with the other squarks. The masses of the squarks and gluinos are assumed to be above 100 GeV. (For experimental bounds see Ref. [6]). The squark and gluino masses are defined as pole masses.

The diagrams for the squark and gluino decays are displayed in Fig. 1. While (a) represents the Born diagrams for the two decay modes, the self-energy diagrams are shown in (b), vertex corrections in (c), and hard-gluon radiation in (d). In (c) and (d) we only give the squark-decay diagrams, as the gluino and squark decay processes are related to each other by crossing.

The ultra-violet, infrared, and collinear divergences have been regularized by switching to $n = 4 + \varepsilon$ dimensions. The actual calculation has been carried out in two schemes:

(i) It is well-known that dimensional reduction \overline{DR} [7] preserves supersymmetry at least to one-loop. This scheme is hence an obvious candidate for performing the renormalization; some technical difficulties in handling the factorization of collinear singularities, however, still demand a proper understanding [8].

(ii) From a technical point of view, the \overline{MS} renormalization scheme [9] is easier to handle in general. However, by introducing a mismatch between the number of gauge-boson and gaugino degrees of freedom in $n \neq 4$ dimensions, the scheme violates supersymmetry explicitly. In particular, the $q\tilde{q}\tilde{g}$ Yukawa coupling \hat{g}_s , which by supersymmetry should coincide with the qqg gauge coupling g_s , deviates from g_s by a finite amount at the one-loop order. Requiring the physical amplitudes to be independent of the renormalization scheme, a shift between the bare Yukawa and gauge couplings must be introduced in the \overline{MS} scheme [10],

$$\hat{g}_s = g_s \left[1 + \frac{\alpha_s}{4\pi} \left(\frac{2}{3}C_A - \frac{1}{2}C_F \right) \right] \quad (3)$$

which effectively subtracts the contributions of the false, non-supersymmetric degrees of freedom (also called ε scalars); $C_A = 3$ and $C_F = 4/3$ are the Casimir invariants of the $SU(3)$ gauge group.

Taking into account this shift in the \overline{MS} scheme, we find that all results are identical with the results obtained within the \overline{DR} scheme bearing in mind the relation between the gauge couplings in the two schemes. This comparison provides non-trivial consistency checks of the one-loop SUSY-QCD corrections.

The need for introducing a finite shift is best demonstrated for the effective $q\tilde{q}\tilde{g}$ Yukawa coupling, which must be equal to the qqg gauge coupling in a supersymmetric world with massless gauginos/gluons and equal-mass squarks/quarks. For the sake of simplicity we define the effective couplings $g_s^{eff}(Q^2)$ and $\hat{g}_s^{eff}(Q^2)$ in the limit of on-shell squarks/quarks and almost on-shell gluinos/gluons with virtuality $Q^2 \ll m_{\tilde{q}}^2 = m_q^2$. [In this limit the couplings do not involve gauge-dependent terms.]

First we consider the corrections of the couplings

$$g_s^{eff}(Q^2) = g_s(1 + \delta) \quad \text{and} \quad \hat{g}_s^{eff}(Q^2) = \hat{g}_s(1 + \hat{\delta}) \quad (4)$$

in the \overline{MS} scheme. By adding the contributions of the external self-energies and the charge renormalization to the vertex corrections [all given explicitly in the appendix], we find the

following results¹:

$$\overline{MS}: \quad \hat{\delta}(q\tilde{q}\tilde{g}) = \frac{\alpha_s}{4\pi} \left\{ C_A \left[\frac{2}{\varepsilon} - \frac{1}{2} \log \left(\frac{Q^2}{m_{\tilde{q}}^2} \right) + \frac{1}{2} \right] + \frac{C_F}{2} \right\} \quad (5)$$

$$\delta(qqg) = \frac{\alpha_s}{4\pi} C_A \left[\frac{2}{\varepsilon} - \frac{1}{2} \log \left(\frac{Q^2}{m_{\tilde{q}}^2} \right) + \frac{7}{6} \right] \quad (6)$$

The difference between δ and $\hat{\delta}$ is indeed compensated by the finite shift introduced in Eq. (3). As a result, the couplings $g_s^{eff}(Q^2)$ and $\hat{g}_s^{eff}(Q^2)$ agree with each other to one-loop, as required by supersymmetry. The same observation can be made in the \overline{DR} scheme. In this scheme we find

$$\overline{DR}: \quad \hat{\delta}(q\tilde{q}\tilde{g}) = \frac{\alpha_s}{4\pi} C_A \left[\frac{2}{\varepsilon} - \frac{1}{2} \log \left(\frac{Q^2}{m_{\tilde{q}}^2} \right) + 1 \right] \quad (7)$$

$$\delta(qqg) = \frac{\alpha_s}{4\pi} C_A \left[\frac{2}{\varepsilon} - \frac{1}{2} \log \left(\frac{Q^2}{m_{\tilde{q}}^2} \right) + 1 \right] \quad (8)$$

As anticipated, the \overline{DR} renormalization scheme preserves supersymmetry and guarantees that the gauge and Yukawa couplings also coincide to one-loop order in the supersymmetric limit. (Note the difference between the effective gauge couplings in the \overline{MS} and \overline{DR} scheme, $(\alpha_s/4\pi) \times C_A/6$; see also Ref. [10, 11]).

3 Results

At the Born level, the partial widths of the decay processes (1) and (2) are given by

$$\Gamma_0(\tilde{q} \rightarrow \tilde{g} + q) = \frac{\alpha_s C_F}{2} \frac{(m_{\tilde{q}}^2 - m_{\tilde{g}}^2)^2}{m_{\tilde{q}}^3} \quad (9)$$

$$\Gamma_0(\tilde{g} \rightarrow \tilde{q} + q, \tilde{q} + \bar{q}) = 4n_f \frac{\alpha_s}{8} \frac{(m_{\tilde{g}}^2 - m_{\tilde{q}}^2)^2}{m_{\tilde{g}}^3} \quad (10)$$

It is implicitly understood in the subsequent formulae, that all flavors, helicities and \mathcal{C} related modes for the gluino decays are summed up. Adding up virtual corrections and gluon bremsstrahlung, the final result including one-loop SUSY-QCD corrections may be written in the form:

$$\Gamma(\tilde{q}) = \Gamma_0(\tilde{q}) \left\{ 1 + \frac{\alpha_s}{\pi} [C_A F_A + C_F F_F + n_f F_f + F_t + F_{ren} + F_{dec}] \right\} \quad (11)$$

$$\Gamma(\tilde{g}) = \Gamma_0(\tilde{g}) \left\{ 1 + \frac{\alpha_s}{\pi} [C_A (F_A - \pi^2) + C_F (F_F + \pi^2) + n_f F_f + F_t + F_{ren} + F_{dec}] \right\} \quad (12)$$

¹The remaining $1/\varepsilon$ poles are associated solely with infrared and collinear singularities, while all ultra-violet singularities are cancelled.

The coefficients F_A etc. are universal functions for both processes, depending only on the respective mass ratios

$$r = \frac{m_{\tilde{g}}^2}{m_{\tilde{q}}^2} \quad \text{and} \quad t = \frac{m_{\tilde{g}}^2}{m_t^2}$$

The difference between the formulae (11) and (12) for the two processes is the result of the analytic continuation of the universal virtual corrections from the region $m_{\tilde{q}} > m_{\tilde{g}}$ to the region $m_{\tilde{g}} > m_{\tilde{q}}$, which gives rise to the π^2 terms. The coefficients read explicitly:

$$\begin{aligned} F_A &= \frac{3}{r-1} \text{Li}_2(1-r) - \frac{r}{r-1} \text{Li}_2(-r) + \frac{5r-6}{12(r-1)} \pi^2 + \frac{59}{24} + \frac{r}{4(r-1)} \\ &\quad + \left[\frac{3+r}{2(r-1)} \log(r) - 2 \right] \log|1-r| + \left[\frac{r(5r-6)}{4(r-1)^2} - \frac{r}{r-1} \log(1+r) \right] \log(r) \\ F_F &= -\frac{2}{r-1} \text{Li}_2(1-r) + \frac{2r}{r-1} \text{Li}_2(-r) + \frac{4-3r}{6(r-1)} \pi^2 + \frac{5}{2} - \frac{r}{2} \\ &\quad + \left[r - \frac{r^2}{2} - \frac{r+1}{r-1} \log(r) \right] \log|1-r| + \left[\frac{2r}{r-1} \log(1+r) - r + \frac{r^2}{2} \right] \log(r) \\ F_f &= -\frac{3}{4r} + \frac{(r-1)(r+3)}{4r^2} \log|1-r| \\ F_t &= \frac{1}{4r} - \frac{1}{4t} \left[1 - \log\left(\frac{r}{t}\right) \right] + \frac{1}{4} \left(\frac{1}{t} - \frac{1}{r} - 1 \right) B_0 + \frac{1}{2} \left(\frac{1}{r} - \frac{1}{t} - 1 \right) B'_0 \end{aligned}$$

with

$$\begin{aligned} B_0 &= \text{Re} \left[2 + x_1 \log(1 - 1/x_1) + x_2 \log(1 - 1/x_2) \right] \\ B'_0 &= \text{Re} \left[-1 + \frac{x_1(1-x_1) \log(1 - 1/x_1) - x_2(1-x_2) \log(1 - 1/x_2)}{x_1 - x_2} \right] \\ x_{1,2} &= \frac{1}{2} \left[1 + \frac{1}{t} - \frac{1}{r} \pm \sqrt{(1 + 1/t - 1/r)^2 - 4/t} \right] \end{aligned}$$

The F_F part represents the supersymmetric version of the abelian vertex and self-energy contributions. The F_f and F_t contributions are due to quark–squark self-energy corrections of the gluino; the gluino–gluon loop is incorporated in F_A . In addition we have introduced the renormalization functions

$$\begin{aligned} F_{ren} &= \frac{3C_A - n_f - 1}{4} \log(\mu_R^2/m_{\tilde{q}}^2) \\ F_{dec} &= \frac{n_f + 1}{12} \log(\mu_R^2/m_{\tilde{q}}^2) + \frac{1}{6} \log(\mu_R^2/m_t^2) + \frac{C_A}{6} \log(\mu_R^2/m_{\tilde{g}}^2) \end{aligned}$$

where μ_R denotes the renormalization scale of the coupling α_s . The second part F_{dec} is added to decouple the heavy particles (top quarks, squarks, gluinos) from the running α_s . [This term may be omitted if the running coupling is adjusted properly].

Characteristic features of the corrections are exemplified in Fig. 2. The three figures in the left column display the width $\tilde{q} \rightarrow \tilde{g}q$, the figures in the right column the width $\tilde{g} \rightarrow \tilde{q}q, \tilde{q}\bar{q}$ for five light quark flavors.

The corrections for the squark decays are moderate. In Fig. 2(a) the Born approximation (LO) and the next-to-leading order (NLO) SUSY-QCD results are displayed for $\mu_R = m_{\tilde{q}}$. The masses are chosen to be $m_{\tilde{q}} = 300$ GeV, $m_{\tilde{g}} \geq 100$ GeV, and $m_t = 180$ GeV. The running coupling $\alpha_s(\mu_R^2)$ is normalized such that $\alpha_s(M_Z^2) = 0.118$. As outlined before, the running of the coupling is defined in next-to-leading order by the standard QCD spectrum with $n_f = 5$ flavors, and the heavy particles are decoupled. The size of the corrections², measured by the ratio Γ_{NLO}/Γ_{LO} in Fig. 2(b), depends on the mass ratio $m_{\tilde{g}}/m_{\tilde{q}}$. With corrections between +30% and +50%, they appear sizable but still under control.

The gluino decays are discussed, in a similar way, in Fig. 2(d) and (e). The corrections are considerably smaller in this case. The dip in the NLO curve is due to the external gluino self-energy, related to the $\tilde{g} \rightarrow \tilde{t}\bar{t}$ threshold in the stop-top loop. The singularities are artificial; they are smoothed out by the strong stop-top interactions and the finite lifetimes of these particles. Including the widths for \tilde{t} and \bar{t} in F_t removes part of the irregularity (see full curves). In view of the small region in parameter space where this effect plays a role, we refrain from a more detailed discussion.

It is evident from the last figures in each column, Fig. 2(c) and (f), in which the variation of the widths with the renormalization scale μ_R is shown, that the NLO corrections improve the stability of the theoretical predictions for the widths significantly. This is the case in particular for the gluino decay width, where a wide and shallow extremum is observed for $\mu_R/m_{\tilde{g}}$ near unity.

To shed more light on these somewhat complicated results, it is interesting to consider two limiting cases. We have considered the massless limit for the particles in the final states, and the threshold effects in the limit of nearly equal masses for squarks and gluinos. For the sake of simplicity, we do not decouple the gluinos and squarks from α_s and we take for illustration also the top mass equal to zero. Setting the scale μ_R equal to the mass of the decaying particle, we find:

²Since Λ_{QCD} is not really well-defined in LO, we have identified α_s in LO with α_s in NLO at the mass scale chosen for comparison.

massless gluinos/squarks in the final state:

$$\begin{aligned}\Gamma(\tilde{q}) &= \Gamma_0(\tilde{q}) \left\{ 1 + \frac{\alpha_s}{\pi} \left[\frac{59}{24} C_A + \left(\frac{5}{2} - \frac{\pi^2}{3} \right) C_F - \frac{n_f + 1}{8} \right] \right\} \\ \Gamma(\tilde{g}) &= \Gamma_0(\tilde{g}) \left\{ 1 + \frac{\alpha_s}{\pi} \left[\left(\frac{65}{24} - \frac{5\pi^2}{12} \right) C_A + \left(\frac{7}{4} + \frac{\pi^2}{6} \right) C_F \right] \right\}\end{aligned}$$

threshold limit $m_{\tilde{q}} \approx m_{\tilde{g}}$:

$$\begin{aligned}\Gamma(\tilde{q}) &= \Gamma_0(\tilde{q}) \left\{ 1 + \frac{\alpha_s}{\pi} \left[\frac{3C_F}{2} \log \left(\frac{m_{\tilde{q}}^2}{m_{\tilde{q}}^2 - m_{\tilde{g}}^2} \right) - \frac{3(n_f + 1)}{4} + \frac{5C_A}{6} + 4C_F + \frac{\pi^2 C_A}{2} - \frac{2\pi^2 C_F}{3} \right] \right\} \\ \Gamma(\tilde{g}) &= \Gamma_0(\tilde{g}) \left\{ 1 + \frac{\alpha_s}{\pi} \left[\frac{3C_F}{2} \log \left(\frac{m_{\tilde{g}}^2}{m_{\tilde{g}}^2 - m_{\tilde{q}}^2} \right) - \frac{3(n_f + 1)}{4} + \frac{5C_A}{6} + 4C_F - \frac{\pi^2 C_A}{2} + \frac{\pi^2 C_F}{3} \right] \right\}\end{aligned}$$

The different size of the corrections for squark and gluino decays is nicely illustrated by the limiting case of massless particles in the final state. The driving term for squark decays is the large C_A contribution while other color structures play a minor role. For gluino decays, however, the different π^2 terms, induced by the vertex correction for $m_{\tilde{g}} > m_{\tilde{q}}$, lead to a destructive interference between the reduced (negative) C_A contribution and the enhanced (positive) contribution from the other color structures. As a result the SUSY-QCD corrections to gluino decays are significantly smaller than the corrections for squark decays.

In addition to the proof that the effective Yukawa and gauge couplings are identical in the limit of exact supersymmetry, we have performed several other consistency checks. We have shown, by using a small gluon mass in the \overline{DR} scheme, that infrared and final-state collinear divergences do not give rise to finite differences between the \overline{MS} and the \overline{DR} schemes. The limiting case $m_{\tilde{g}} \rightarrow 0$ discussed in the previous paragraph has been extracted from the general formulae and it has been compared with an *ab initio* rederivation of the squark width (which can be calculated much more easily in this limit). Finally, by limiting the calculation to the subset of abelian diagrams (*i.e.* the C_F part), we have reproduced the results of Ref. [3] for SUSY-QCD corrected squark decays to quarks and photinos after having corrected the sign of the vertex correction Eq. (19) in Ref. [3].

Acknowledgement

We gratefully acknowledge a clarifying communication on the sign of the $q\tilde{q}\tilde{\gamma}$ vertex correction by K. Hikasa. W.B. thanks the DESY Theory Group for the warm hospitality extended to him during a visit.

Appendix

In this appendix we present the exact supersymmetric one-loop corrections to the $q\tilde{q}\tilde{g}$ and qqg couplings, Eq. (4), discussed in Sect. 2 for $Q^2 \ll m_{\tilde{q}}^2 = m_q^2$. The corrections are given in both the \overline{MS} and the \overline{DR} renormalization schemes.

\overline{MS} Renormalization Scheme:

vertex corrections

$$\begin{aligned} (q\tilde{q}\tilde{g}) \quad \hat{\delta}_V &= \frac{\alpha_s}{4\pi} \left\{ C_A \left[-\frac{2}{\varepsilon} - \log \left(\frac{Q^2}{m_{\tilde{q}}^2} \right) + 1 \right] + C_F \left[-\frac{6}{\varepsilon} + 6 \right] \right\} \\ (qqg) \quad \delta_V &= \frac{\alpha_s}{4\pi} C_F \left[-\frac{8}{\varepsilon} + 7 \right] \end{aligned}$$

wave-function renormalization

$$\begin{aligned} (Z_q - 1)/2 &= \frac{\alpha_s}{4\pi} C_F \left[\frac{4}{\varepsilon} - \frac{7}{2} \right] \\ (Z_{\tilde{q}} - 1)/2 &= \frac{\alpha_s}{4\pi} C_F \left[\frac{2}{\varepsilon} - 2 \right] \\ (Z_g - 1)/2 &= \frac{\alpha_s}{4\pi} \left\{ C_A \left[-\frac{1}{\varepsilon} - \frac{1}{2} \log \left(\frac{Q^2}{m_{\tilde{q}}^2} \right) + \frac{7}{6} \right] + (n_f + 1) \frac{1}{\varepsilon} \right\} \\ (Z_{\tilde{g}} - 1)/2 &= \frac{\alpha_s}{4\pi} \left\{ C_A \left[\frac{1}{\varepsilon} + \frac{1}{2} \log \left(\frac{Q^2}{m_{\tilde{q}}^2} \right) - \frac{1}{2} \right] + (n_f + 1) \frac{1}{\varepsilon} \right\} \end{aligned}$$

charge renormalization

$$Z_{g_s} - 1 = Z_{\hat{g}_s} - 1 = \frac{\alpha_s}{4\pi} \left[C_A \frac{3}{\varepsilon} - (n_f + 1) \frac{1}{\varepsilon} \right]$$

\overline{DR} Renormalization Scheme:

vertex corrections

$$\begin{aligned} (q\tilde{q}\tilde{g}) \quad \hat{\delta}_V &= \frac{\alpha_s}{4\pi} \left\{ C_A \left[-\frac{2}{\varepsilon} - \log \left(\frac{Q^2}{m_{\tilde{q}}^2} \right) + 2 \right] + C_F \left[-\frac{6}{\varepsilon} + 6 \right] \right\} \\ (qqg) \quad \delta_V &= \frac{\alpha_s}{4\pi} C_F \left[-\frac{8}{\varepsilon} + 8 \right] \end{aligned}$$

wave-function renormalization

$$(Z_q - 1)/2 = \frac{\alpha_s}{4\pi} C_F \left[\frac{4}{\varepsilon} - 4 \right]$$

$$(Z_{\hat{q}} - 1)/2 = \frac{\alpha_s}{4\pi} C_F \left[\frac{2}{\varepsilon} - 2 \right]$$

$$(Z_g - 1)/2 = \frac{\alpha_s}{4\pi} \left\{ C_A \left[-\frac{1}{\varepsilon} - \frac{1}{2} \log \left(\frac{Q^2}{m_{\hat{q}}^2} \right) + 1 \right] + (n_f + 1) \frac{1}{\varepsilon} \right\}$$

$$(Z_{\hat{g}} - 1)/2 = \frac{\alpha_s}{4\pi} \left\{ C_A \left[\frac{1}{\varepsilon} + \frac{1}{2} \log \left(\frac{Q^2}{m_{\hat{q}}^2} \right) - 1 \right] + (n_f + 1) \frac{1}{\varepsilon} \right\}$$

charge renormalization

$$Z_{g_s} - 1 = Z_{\hat{g}_s} - 1 = \frac{\alpha_s}{4\pi} \left[C_A \frac{3}{\varepsilon} - (n_f + 1) \frac{1}{\varepsilon} \right]$$

References

- [1] W. Beenakker, R. Höpker, M. Spira and P. M. Zerwas, *Phys. Rev. Lett.* **74** (1995) 2905, and *Z. Phys.* **C69** (1995) 163.
- [2] A. Arhrib, M. Capdequi-Peyranere and A. Djouadi, *Phys. Rev.* **D52** (1995) 1404.
- [3] K. Hikasa and Y. Nakamura, Tohoku preprint *TU-475* (*hep-ph/9501382*).
- [4] A. Bartl, H. Eberl, K. Hidaka, T. Kon, W. Majerotto and Y. Yamada, Vienna preprint *UWTHPH-1995-26* (*hep-ph/9508283*).
- [5] A. Bartl, H. Eberl, K. Hidaka, T. Kon, W. Majerotto and Y. Yamada, Vienna preprint *UWTHPH-1995-35* (*hep-ph/9511385*).
- [6] F. Abe *et al.*, CDF Coll., *Phys. Rev. Lett.* **75** (1995) 613; S. Abachi *et al.*, D0 Coll., *Phys. Rev. Lett.* **75** (1995) 618.
- [7] W. Siegel, *Phys. Lett.* **B84** (1979) 193; D.M. Capper, D.R.T. Jones and P. van Nieuwenhuizen, *Nucl. Phys.* **B167** (1980) 479.
- [8] W. Beenakker, H. Kuijf, W.L. van Neerven and J. Smith, *Phys. Rev.* **D40** (1989) 54.
- [9] G. 't Hooft and M. Veltman, *Nucl. Phys.* **B44** (1972) 189; W.A. Bardeen, A.J. Buras, D.W. Duke and T.W. Muta, *Phys. Rev.* **D18** (1978) 3998.

- [10] S.P. Martin and M.T. Vaughn, *Phys. Lett.* **B318** (1993) 331.
- [11] G.A. Schuler, S. Sakakibara and J.G. Körner, *Phys. Lett.* **B194** (1987) 125.

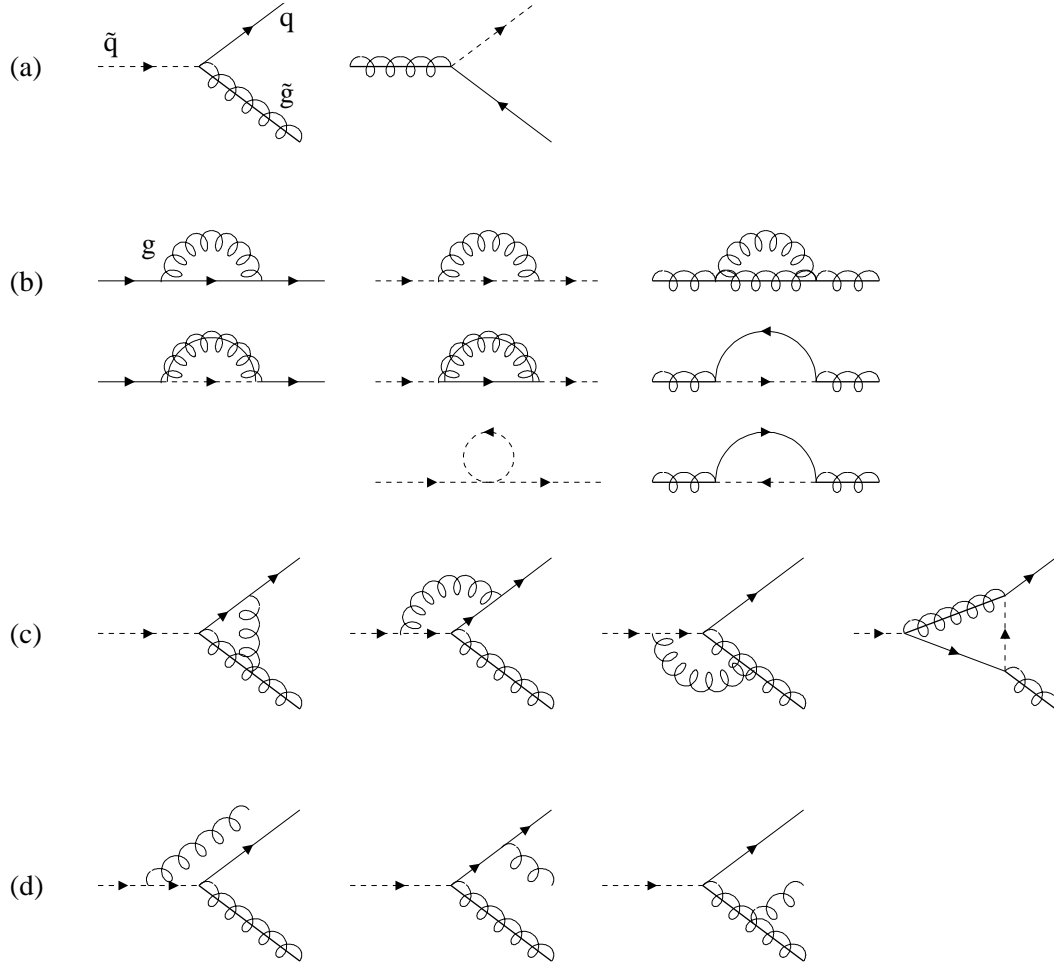


Figure 1: The Feynman diagrams for squark and gluino decays. (a) Born diagram for both decay modes; (b) quark, squark, and gluino self-energies; (c) vertex corrections for squark decays; (d) gluon radiation for squark decays. The diagrams of type (c) and (d) for gluino decays can be generated by rotating the diagrams for squark decays.

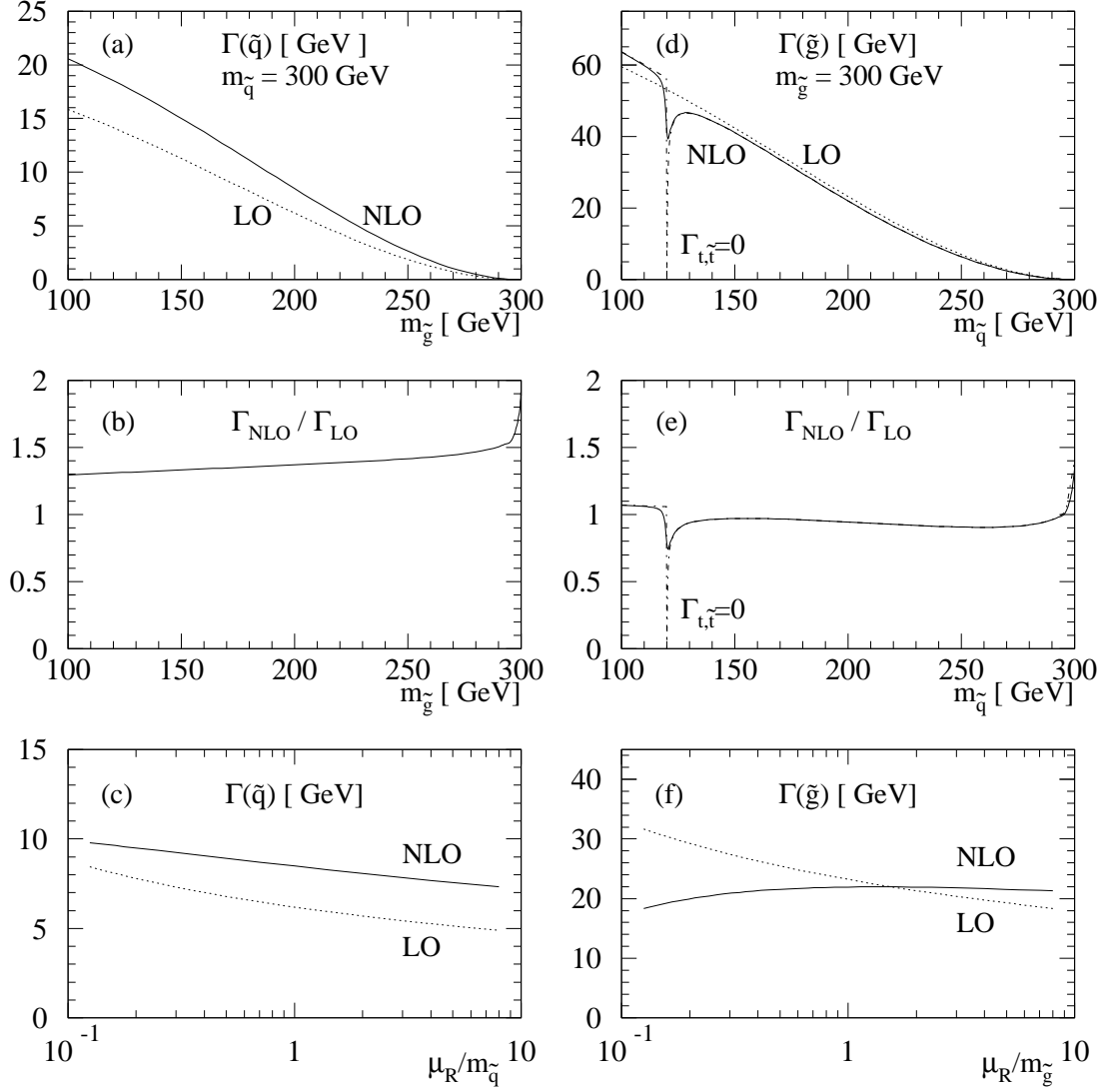


Figure 2: The SUSY-QCD corrections to squark and gluino decays. (a) The decay rate for squarks ($m_{\tilde{q}} = 300$ GeV) in LO (dashed curve) and in NLO (solid curve) for $\mu_R = m_{\tilde{q}}$; (b) the ratio of the decay rate for squarks in NLO and in LO for $\mu_R = m_{\tilde{q}}$; (c) the scale dependence of the decay rate for squarks in LO and in NLO ($m_{\tilde{q}} = 200$ GeV). (d-f): The same quantities for gluino decays with interchanged, but otherwise identical mass parameters. The long-dashed curve in (d) and (e) represents NLO results without taking into account non-zero widths for stop and top.